

# Analytic formulae for non-local magic in bipartite systems of qutrits and ququints

Giorgio Busoni,<sup>\*</sup> John Gargalionis,<sup>†</sup> Ewan N. V. Wallace,<sup>‡</sup> and Martin J. White<sup>§</sup>  
University of Adelaide, ARC Centre of Excellence for Dark Matter Particle Physics & CSSM,  
Department of Physics, Adelaide SA 5000 Australia  
(Dated: March 11, 2026)

We conjecture analytic expressions for the non-local magic of bipartite pure qudit states of prime local dimension. Our construction relies on the Schmidt-aligned state attaining the minimum over local unitaries, a hypothesis that we support with numerical evidence for pairs of qutrits and ququints. For composite local dimensions, we find that the analogous expressions do not in general reproduce the global minimum, but can still provide computationally cheap approximations to the non-local magic. We also find that relations between non-local magic and entanglement diagnostics that hold for two qubits generally do not extend to qutrit and higher-dimensional systems.

## I. INTRODUCTION

Quantum computation based on higher-dimensional systems, or *qudits*, has recently gained increasing attention as a route to enhance gate efficiency, noise resilience, and information density [1]. Among these, qutrits (local dimension  $N = 3$ ) and ququints ( $N = 5$ ) have emerged as leading candidates for near-term implementations. In any quantum computational system, identifying and quantifying the non-stabiliser content of states is essential, since non-stabiliser, or *magic*, states represent a fundamental resource enabling universal quantum computation beyond the Clifford group [2–24].

Several approaches have been developed to quantify magic, e.g. [5, 16, 25, 26]. Recently, a basis-independent measure of non-stabiliserness, the non-local nonstabiliserness, has been introduced [27–30]. It is defined through the minimisation of a magic monotone  $M$  over all local unitary transformations acting independently on two subsystems  $A$  and  $B$ :

$$\mathcal{M}_{AB}(|\Psi_{AB}\rangle) = \min_{U_A \otimes U_B} [M(U_A \otimes U_B |\Psi_{AB}\rangle)] , \quad (1)$$

where we use  $\mathcal{M}$  for the non-local nonstabiliserness, which we here refer to as the non-local magic (NLM). This quantity shares the same symmetries as entanglement measures, making it a resource of central importance for quantum computation. Indeed, for a system of two pure qubits it can be directly related to the flatness of the entanglement spectrum [31, 32], and so a non-zero value for  $\mathcal{M}$  signals the presence of both magic and entanglement in the state. For bipartite pure qubit systems, the minimisation over local unitaries admits an analytic solution in terms of invariants of the  $U(2) \otimes U(2)$  group, but an analogous formulation for qudits with local dimension  $N > 2$  has remained unavailable.

In this work, we generalise the analytic construction of the NLM to bipartite pure qudit systems of prime dimension. Our approach is to expand the density matrix on

the basis of tensor-product generalised Pauli operators and identify quartic invariants of these coefficients under local unitary transformations. From this we derive a closed analytic expression that we show to be equivalent to the NLM for systems of two qutrits and two ququints. Our derivation assumes that the NLM minimum is attained by Schmidt-aligned states, a hypothesis we dub *Schmidt attainment*; we do not prove this assumption, but support it with a dedicated numerical comparison against direct optimisation over  $U_A \otimes U_B$  for  $N = 3, 5$ . This result supports the conjecture that the method extends to all prime-dimensional qudits. In contrast, for composite dimensions such as  $N = 4$ , the Schmidt-aligned ansatz is not globally optimal throughout parameter space, although we advocate that it is a good and computationally cheap approximation. We also report the spectra of the reduced density matrices corresponding to minimal and maximal NLM values for  $N = 3, 5$ , providing a geometric interpretation of the non-stabiliserness landscape in these cases.

The results presented here offer a rapid, analytic and basis-independent means to evaluate non-stabiliserness in prime-dimensional bipartite pure systems of low dimension, relevant to current experimental and theoretical efforts in qudit-based quantum computing, and recent applications in particle-physics contexts where fermion flavours are modelled as qutrits [33, 34].

The remainder of the paper is structured as follows. In Sec. II we phrase the bipartite qubit case studied in Ref. [27] in the language of invariants, preparing the reader for the extension to higher-dimensional qudits presented in Sec. III. In Sec. IV we present closed-form formulae and analyse the  $N \leq 5$  cases, before presenting our conclusions in Sec. V. Appendix A describes our numerical experiments validating the Schmidt-attainment hypothesis.

<sup>\*</sup> giorgio.busoni@adelaide.edu.au

<sup>†</sup> john.gargalionis@adelaide.edu.au

<sup>‡</sup> ewan.n.wallace@adelaide.edu.au

<sup>§</sup> martin.white@adelaide.edu.au

## II. TWO-QUBIT NON-LOCAL MAGIC FROM LOCAL-UNITARY INVARIANTS

We begin with a pure two-qubit state

$$|\psi\rangle = \sum_{j,k=0}^1 x_{jk} |jk\rangle ; \quad (2)$$

such a state always admits a Schmidt decomposition of the form

$$|\psi_\lambda\rangle = \lambda_0 |00\rangle + \lambda_1 |11\rangle , \quad (3)$$

where  $\lambda_i$  are the Schmidt coefficients, which can always be taken to be real and positive.

For a pure state the eigenvalues of the reduced density matrix encode the Schmidt coefficients. Indeed, from a practical point of view the Schmidt decomposition is obtained by finding the eigenvalues of the reduced density matrix of one of the subsystems. For a two-qubit system with subsystems  $A$  and  $B$ , this is equivalent to

$$\rho_X \sim \begin{bmatrix} \lambda_0^2 & 0 \\ 0 & \lambda_1^2 \end{bmatrix} , \quad (4)$$

where  $\rho_X$  represents the reduced density matrix of subsystem  $X$ , for  $X \in \{A, B\}$ . Each normalised reduced density matrix satisfies

$$\text{Tr } \rho_X = 1 \quad (5)$$

and transforms as

$$\rho_X \rightarrow U_X^\dagger \rho_X U_X \quad (6)$$

under  $U_A \otimes U_B$  transformations. Since the normalisation condition fixes the trace, there is a single invariant degree of freedom that can be taken to be the determinant of the reduced density matrix of Eq. (4):

$$e_2 \equiv \det \rho_A = \det \rho_B . \quad (7)$$

Since the density matrix is Hermitian, it can be decomposed by projecting it over the set of matrices  $\sigma_{\mu\nu} = \sigma_\mu \otimes \sigma_\nu$ , where

$$\sigma_\mu \equiv \{\mathbb{I}, \sigma_x, \sigma_y, \sigma_z\} \quad (8)$$

and  $\mu \in \{0, 1, 2, 3\}$ , which form a complete basis for  $4 \times 4$  Hermitian matrices. Concretely, we take this projection to be

$$\rho = \frac{\sigma_{\mu\nu} \text{Tr} [\sigma_{\mu\nu} \rho]}{\text{Tr} [\sigma_{\mu\nu} \sigma_{\mu\nu}]} = \frac{1}{4} \sigma_{\mu\nu} \text{Tr} [\sigma_{\mu\nu} \rho] \equiv \frac{1}{4} R_{\mu\nu} \sigma_{\mu\nu} , \quad (9)$$

where we understand an implied sum over repeated indices, and we have defined [35, 36]

$$R_{\mu\nu} \equiv \text{Tr} [\sigma_{\mu\nu} \rho] . \quad (10)$$

The  $R_{\mu\nu}$  are real as both  $\rho$  and  $\sigma_{\mu\nu}$  are Hermitian; these components transform in the same way as  $\sigma_{\mu\nu} = \sigma_\mu \otimes \sigma_\nu$

under  $U_A \otimes U_B$  transformations. As  $\mathbb{I}$  is an  $\text{SU}(2)$  singlet and  $\sigma_i$ , with  $i \in \{x, y, z\}$ , transforms like a triplet,  $R_{\mu\nu}$  can be decomposed as

$$R_{\mu\nu} = \begin{bmatrix} 1 & a^\top \\ b & T \end{bmatrix} , \quad (11)$$

where, in the sense of  $\text{SU}(2) \times \text{SU}(2)$  representations,  $a \in (\mathbf{1}, \mathbf{3})$ ,  $b \in (\mathbf{3}, \mathbf{1})$ , and  $T \in (\mathbf{3}, \mathbf{3})$ , so they transform as  $a \rightarrow O_A a$ ,  $b \rightarrow O_B b$  and  $T \rightarrow O_B T O_A^\top$ , where the  $O_X$  are elements of  $\text{SO}(3)$  that depend on  $U_X$ . Due to the fact that  $\text{SU}(2)$  is a double cover of  $\text{SO}(3)$ , for any rotation  $O_X$  there is always a unitary transformation  $U_X$  of the qubit that gives such an  $O_X$  for  $R_{\mu\nu}$ . This guarantees that the matrix  $T$  can always be diagonalised with the right choices of  $U_A$  and  $U_B$ .

Indeed, we highlight that the basis defined by the Schmidt decomposition diagonalises the matrix  $T$ . If we parametrise

$$\lambda_0 = \cos \theta, \quad \lambda_1 = \sin \theta , \quad (12)$$

one gets

$$e_2 = \frac{1}{4} \sin^2 (2\theta) , \quad (13)$$

for the determinant of the reduced density matrices, and the subcomponents of  $R_{\mu\nu}$  from Eq. (11) take the form

$$a = b = \begin{bmatrix} 0 \\ 0 \\ \cos 2\theta \end{bmatrix} \quad (14)$$

and

$$T = \begin{bmatrix} \sin 2\theta & 0 & 0 \\ 0 & -\sin 2\theta & 0 \\ 0 & 0 & 1 \end{bmatrix} . \quad (15)$$

We proceed by adopting the second stabiliser Rényi entropy as our magic monotone [26]. In this case, the NLM can be expressed as

$$\mathcal{M}_{AB} = \min_{U_A \otimes U_B} \left( -\ln \frac{\sum_{\mu\nu} \text{Tr} [\sigma_{\mu\nu} \rho]^4}{\sum_{\mu\nu} \text{Tr} [\sigma_{\mu\nu} \rho]^2} \right) , \quad (16)$$

which can be written in terms of the coefficients  $R_{\mu\nu}$ :

$$\mathcal{M}_{AB} = \min_{U_A \otimes U_B} \left( -\ln \frac{\sum_{\mu\nu} |R_{\mu\nu}|^4}{4} \right) , \quad (17)$$

where we have also specialised to the case of a pure state. The minimum over  $U_A \otimes U_B$  occurs when

$$\sum_{\mu,\nu} R_{\mu\nu}^4 \quad (18)$$

is maximised,<sup>1</sup> and this maximum is attained in the Schmidt basis, where  $T$  is diagonal [27].<sup>2</sup>

For the Schmidt-form state  $|\psi\rangle = \cos\theta |00\rangle + \sin\theta |11\rangle$ , there are only six non-zero Pauli expansion coefficients  $R_{\mu\nu}$ :  $R_{00} = R_{33} = 1$ ,  $R_{30} = R_{03} = \cos 2\theta$ , and  $R_{11} = -R_{22} = \sin 2\theta$ . Evaluating the objective gives  $\sum_{\mu\nu} R_{\mu\nu}^4 = 4 - \sin^2(4\theta)$ , which can be written in terms of the local-unitary invariant  $e_2 = \det \rho_A = \frac{1}{4} \sin^2(2\theta)$  to give

$$\mathcal{M} = -\ln(1 - 4e_2 + 16e_2^2) \quad (19)$$

for the NLM for a two-qubit system.

### III. EXTENSION TO PRIME-DIMENSIONAL QUDITS

In this section we extend the invariant-based construction of non-local magic from two qubits to bipartite systems of local dimension  $N$ , again specialising to the case of pure states. For  $N = 3, 5$ , we proceed under the Schmidt-attainment hypothesis: the global NLM minimum over local unitaries is attained by Schmidt-aligned states. We provide numerical evidence for this in Appendix A. Accordingly, the resulting closed-form expressions to be introduced in Sec. IV should be interpreted as conjectured formulae for prime  $N$ . Throughout this section we use  $X \in \{A, B\}$  as a shorthand to label the subsystems  $A$  and  $B$ .

We begin with a general pure state

$$|\psi\rangle = \sum_{j,k=0}^{N-1} x_{jk} |jk\rangle, \quad (20)$$

which always admits a Schmidt decomposition

$$|\psi\rangle = \sum_{i=0}^{N-1} \lambda_i |ii\rangle, \quad (21)$$

where the Schmidt coefficients  $\lambda_i$  can be chosen real and non-negative.

<sup>1</sup> Recall that  $R_{\mu\nu} \in \mathbb{R}$ .

<sup>2</sup> A useful way to see this is to decompose the objective according to Eq. (11). The scalar component  $R_{00} = 1$  is invariant. The vectors  $a_i = R_{0i}$  and  $b_i = R_{i0}$  transform under local unitaries as SO(3) vectors, so their Euclidean norms are invariant. For fixed norm, the quartic sum  $\sum_i a_i^4$  is maximised when only one component is non-zero, and likewise for  $\sum_i b_i^4$ ; this is exactly what happens in the Schmidt basis. Similarly, the correlation-matrix elements  $R_{ij} = T_{ij}$  can be written as  $\sum_k (O_B)_{ik} l_k (O_A)_{jk}$  for suitable choices of  $U_A$  and  $U_B$ , where  $l_k$  are the singular values of  $T$ , which are invariants. The orthogonality constraints on  $O_A$  and  $O_B$  imply that mixing the singular-value weight across several entries cannot increase the sum  $\sum_{ij} T_{ij}^4 = \sum_{ij} [\sum_k (O_B)_{ik} l_k (O_A)_{jk}]^4$ , and the quartic sum is therefore maximised when  $T$  is diagonal. Thus the maxima of all sectors are realised simultaneously in the Schmidt basis, yielding the global maximum of Eq. (18).

As in Sec. II, local unitary transformations  $U_A \otimes U_B \in \text{SU}(N) \otimes \text{SU}(N)$  preserve the spectrum of the reduced density matrices, hence the  $\rho_X$  have eigenvalues  $\lambda_i^2$ .<sup>3</sup> For  $N > 2$ , the reduced spectrum contains  $N - 1$  independent invariants (after the normalisation constraint  $\text{Tr} \rho_X = 1$ ); our strategy is therefore to organise these invariants, rewrite the relevant fourth-order correlator in a generalised Pauli basis, and then identify the structure that controls the NLM minimisation.

Generalising the notation from the previous section, we define

$$p_n \equiv \text{Tr}(\rho_X^n), \quad (22)$$

$$e_N \equiv \det \rho_X, \quad (23)$$

which are invariants under local unitary transformations. To express these in terms of Schmidt coefficients, we introduce symmetric and cyclic sums: for a list of exponents  $a = (a_1, \dots, a_N)$ , we have

$$s_{a_1 \dots a_N} \equiv \sum_{\pi \in S_N} \prod_{j=1}^N \lambda_{\pi(j)}^{a_j}, \quad (24)$$

$$c_{a_1 \dots a_N} \equiv \sum_{\pi \in C_N} \prod_{j=1}^N \lambda_{\pi(j)}^{a_j}, \quad (25)$$

where  $S_N$  is the permutation group and  $C_N$  its cyclic subgroup. These represent sums over all permutations of the Schmidt-coefficient labels (for  $S_N$ ) and over cyclic permutations of those labels (for  $C_N$ ). Adopting notation that omits zero exponents when unambiguous, e.g.  $s_{200} = s_2$ , the corresponding relations are

$$p_n = \sum_{i=0}^{N-1} \lambda_i^{2n} = s_{2n} = c_{2n}, \quad (26)$$

$$e_N = \prod_{i=0}^{N-1} \lambda_i^2 = \underbrace{s_{2 \dots 2}}_{N \text{ times}} = \frac{1}{N} \underbrace{c_{2 \dots 2}}_{N \text{ times}}. \quad (27)$$

Moreover,

$$p_{1/2} = \text{Tr}(\sqrt{\rho_X}) = \sum_{i=0}^{N-1} \lambda_i = s_1 = c_1, \quad (28)$$

where  $\sqrt{\rho_X}$  denotes the positive square root of  $\rho_X$ , which is well-defined because  $\rho_X$  is Hermitian and positive semidefinite.

To connect with the NLM objective, we construct a qudit analogue of the qubit coefficients  $R_{\mu\nu}$  introduced in Sec. II. This requires the usual generalisations of the Pauli operators:

$$X |j\rangle = |j + 1 \bmod N\rangle, \quad Z |j\rangle = \omega^j |j\rangle, \quad (29)$$

<sup>3</sup> We note that the restriction to  $\text{SU}(N)$  here is made without loss of generality, since the omitted  $U(1)$  factors contribute only a global phase.

where  $\omega = e^{2\pi i/N}$ , so that  $ZX = \omega XZ$ . The two-qudit operator basis is then

$$P_{abcd} \equiv (X^a Z^b) \otimes (X^c Z^d), \quad (30)$$

with  $a, b, c, d \in \{0, \dots, N-1\}$ .<sup>4</sup> Expanding  $\rho$  on this basis gives

$$\rho = \frac{1}{N^2} \sum_{a,b,c,d} t_{abcd} P_{abcd}, \quad (31)$$

where

$$t_{abcd} \equiv \text{Tr}(\rho P_{abcd}) = \sum_{j,k=0}^{N-1} x_{jk} x_{j+a,k+c}^* \omega^{bj+dk}. \quad (32)$$

This allows us to write the NLM minimand as

$$- \ln \left( \frac{1}{N^2} \sum_{a,b,c,d} |t_{abcd}|^4 \right), \quad (33)$$

in analogy with Eq. (17). The coefficients  $t_{abcd}$  are then the qudit analogue of the qubit coefficients  $R_{\mu\nu}$ . The key difference is that, unlike  $R_{\mu\nu} \in \mathbb{R}$ , the coefficients  $t_{abcd}$  are generally complex because  $P_{abcd}$  is non-Hermitian for  $N > 2$ .

Under the Schmidt-attainment hypothesis discussed above, we evaluate the correlator in the Schmidt-aligned form  $x_{jk} = \lambda_j \delta_{j,k}$ , which gives

$$t_{abcd} = \sum_{j=0}^{N-1} \lambda_j \lambda_{j+a} \omega^{(b+d)j} \delta_{ac}. \quad (34)$$

The Kronecker delta enforces  $c = a$ , so only those components contribute in Eq. (33). This also gives a block-diagonal structure for  $t$ , with  $N$  blocks of dimension  $N \times N$ . In this case, the argument of the logarithm from Eq. (33) is a useful quantity that we further define for use later:

$$F_N(\lambda) \equiv \frac{1}{N^2} \sum_{a,b,c,d} |\text{Tr}(\rho_\lambda P_{abcd})|^4, \quad (35)$$

where  $\rho_\lambda = |\psi_\lambda\rangle\langle\psi_\lambda|$ . The fourth power of the modulus reads

$$|t_{abcd}|^4 = \sum_{j,k,p,q=0}^{N-1} \lambda_j \lambda_{j+a} \lambda_k \lambda_{k+a} \lambda_p \lambda_{p+a} \lambda_q \lambda_{q+a} \cdot \omega^{(b+d)(j-k+p-q)}. \quad (36)$$

In the remaining sum over  $b$  and  $d$ , the phases are projected by

$$\sum_{b,d=0}^{N-1} \omega^{(b+d)(j-k+p-q)} = N^2 \delta_{j-k+p-q, 0 \pmod{N}}. \quad (37)$$

<sup>4</sup> We omit the customary phase factor in the definition of  $P_{abcd}$ , since it cancels in  $|\text{Tr}(\rho P_{abcd})|^4$ .

After dividing by the normalisation factor  $N^2$ , only combinations satisfying

$$j - k + p - q = 0 \pmod{N} \quad (38)$$

survive. This condition allows one to express  $q$  as a function of the other indices:

$$q = j - k + p \pmod{N}, \quad (39)$$

reducing the inner four-index sum to a triple sum over  $(j, k, p)$ , with an outer sum over  $a$ . The final expression, after performing the sums over  $b, d$ , and  $c$ , is then

$$\sum_{a=0}^{N-1} \sum_{j,k,p=0}^{N-1} \lambda_j \lambda_{j+a} \lambda_k \lambda_{k+a} \lambda_p \lambda_{p+a} \lambda_{j-k+p} \lambda_{j-k+p+a} \quad (40)$$

where all indices are taken modulo  $N$ . Each term corresponds to a cyclic combination of indices, and the remaining sum over  $a$  ensures that only cyclically invariant patterns of the exponents contribute to the final expression.

For fixed Schmidt coefficients  $\lambda = (\lambda_0, \dots, \lambda_{N-1})$ , the value of Eq. (40) is just  $F_N(\lambda)$  from Eq. (35). Since local unitaries include permutations of the Schmidt basis, the Schmidt-attained NLM is obtained by evaluating  $F_N$  over the inequivalent permutations of  $\lambda$  (identifying orderings related by cyclic shifts) and taking the largest value:

$$\mathcal{M}_N = - \ln \left( \max_{\lambda'} F_N(\lambda') \right), \quad (41)$$

where  $\lambda'$  runs over permutations of  $\lambda$  modulo cyclic re-belling.

#### IV. RESULTS FOR $N \leq 5$ AND NUMERICAL ANALYSIS

In the following we present simple formulae for two-qudit systems of low dimension and study the landscape of NLM produced in these cases, in order of increasing local dimension.

The closed-form expressions for the argument of the logarithm entering the NLM in the cases  $N \leq 5$  are listed in Table I. We emphasise that the  $N = 4$  row is only included for reference, and the NLM constructed from the corresponding expression does not reproduce the global local-unitary minimum in general.

For qubits, the corresponding formula reproduces Eq. (19) and the results of Ref. [27]. A proof that the NLM minimum is attained in the Schmidt-aligned form in this case is found in the fact that the matrix  $T$  of Eq. (11) can always be diagonalised by appropriate choices of  $U_A$  and  $U_B$ , owing to the relationship between  $SU(2)$  and  $SO(3)$ . The expression depends only on  $e_2 \in [0, 1/4]$  and therefore satisfies  $3/4 \leq F_2(\lambda) \leq 1$ , which implies

$$0 \leq \mathcal{M}_{N=2} \leq \ln \frac{4}{3}. \quad (42)$$

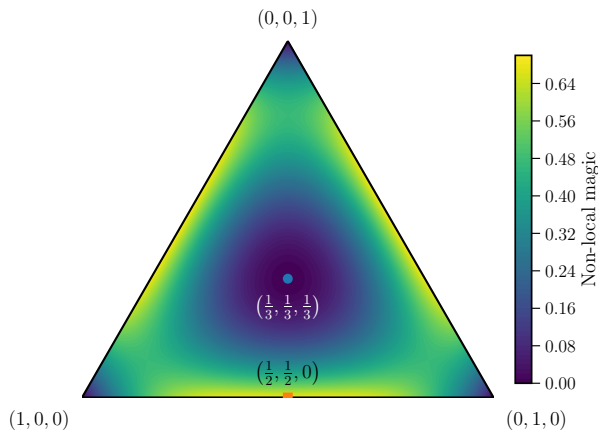


FIG. 1. Non-local magic for two qutrits across the canonical simplex of Schmidt probabilities  $(\lambda_0^2, \lambda_1^2, \lambda_2^2)$ , where  $\sum_i \lambda_i^2 = 1$ . The colour scale shows the non-local magic  $\mathcal{M}_{N=3} = -\ln F_3(\lambda)$ . The plot is symmetric under permutations of  $(\lambda_0^2, \lambda_1^2, \lambda_2^2)$ , appearing as a threefold symmetric pattern over the simplex. The minimum value  $\mathcal{M}_{N=3} = 0$  appears at product-state vertices and at the maximally entangled point  $\lambda_i = 1/\sqrt{3}$  (blue circle), while the maximum  $\mathcal{M}_{N=3} = \ln 2 \approx 0.69$  occurs along rank-two equal spectra, e.g.  $\lambda = (1/\sqrt{2}, 1/\sqrt{2}, 0)$  (orange box), and permutations.

For  $N = 3$  our formula reads

$$F_3(\lambda) = \frac{1}{9} \sum_{a,b,c,d} |t_{abcd}|^4 = 1 - 2p_2 + 2p_2^2 + 4e_3s_1^2, \quad (43)$$

Since  $e_3s_1^2 \geq 0$ , we have  $F_3(\lambda) \geq f(p_2) \equiv 1 - 2p_2 + 2p_2^2$ , whose minimum over the allowed range  $p_2 \in [1/3, 1]$  occurs at  $p_2 = 1/2$  and equals  $f(1/2) = 1/2$ . This bound is saturated by a rank-two equal Schmidt spectrum, e.g.  $\lambda = 2^{-1/2}(1, 1, 0)$ , for which  $e_3 = 0$  and  $p_2 = 1/2$ , and thus  $F_{3,\min} = 1/2$ . Conversely,  $F_3(\lambda) = 1$  (and hence  $\mathcal{M}_{N=3} = 0$ ) both for product states, where  $p_2 = 1$  and  $e_3 = 0$ , and for the maximally entangled spectrum  $\lambda_i = 1/\sqrt{3}$ , where  $p_2 = 1/3$  and  $e_3s_1^2 = 1/9$ . The non-local magic in two qutrits therefore satisfies

$$0 \leq \mathcal{M}_{N=3} \leq \ln 2. \quad (44)$$

The dependence of the non-local magic on the Schmidt coefficients is visualised in Fig. 1 for the qutrit case. We use Schmidt probabilities  $\lambda_i^2$  as canonical simplex coordinates, with  $\sum_i \lambda_i^2 = 1$ . We map these to Cartesian coordinates through

$$(x, y) = (\lambda_1^2 + \frac{1}{2}\lambda_2^2, \frac{\sqrt{3}}{2}\lambda_2^2), \quad (45)$$

so the vertices  $(1, 0, 0)$ ,  $(0, 1, 0)$ ,  $(0, 0, 1)$  form an equilateral triangle. The landscape exhibits the expected overall  $S_3$  permutation symmetry under relabelling of Schmidt components, and the aforementioned pattern of extrema in the non-local magic is clearly visible.

For systems of two ququints, we likewise find that the minimum allowed non-local magic is 0. This is at-

tained for product states, for which one Schmidt coefficient equals 1 and the others vanish, and also for the maximally entangled spectrum  $\lambda_i = 1/\sqrt{5}$ , for which the Schmidt-based expression gives  $F_5(\lambda) = 1$ . To identify the maximum allowed value of the non-local magic, we perform a numerical optimisation over Schmidt spectra. We find a value consistent with  $\ln(27/11)$  to within numerical precision, associated with points along the boundary of Schmidt space corresponding to probabilities  $(\lambda_0^2, \lambda_1^2, \lambda_2^2, \lambda_3^2, \lambda_4^2) = (1/3, 1/3, 1/3, 0, 0)$  and permutations. Thus,

$$0 \leq \mathcal{M}_{N=5} \lesssim \ln \frac{27}{11}, \quad (46)$$

where the upper endpoint is supported numerically. We visualise a slice through this space for fixed  $\lambda_3^2 = \lambda_4^2 = 0$  in Fig. 2. In this slice the central point  $\lambda_0^2 = \lambda_1^2 = \lambda_2^2 = 1/3$  realises the maximal non-local magic.

We briefly comment on the relationship between the non-local magic and entanglement diagnostics. In our notation, the anti-flatness of the entanglement spectrum is

$$\mathcal{F}(|\psi\rangle) = p_3 - p_2^2. \quad (47)$$

For  $n$  qubits, it is known that the *local* magic (as measured by the stabiliser linear entropy [26]) is proportional to the anti-flatness averaged over the Clifford orbit [31]. Moreover, Ref. [32] recently reported an even more basic connection between the NLM and anti-flatness for two-qubit pure states: namely,  $\mathcal{M}_{AB}^{\text{lin}} = 4\mathcal{F}$ , where  $\mathcal{M}_{AB} = -\ln(1 - \mathcal{M}_{AB}^{\text{lin}})$ . This is readily proved in our formalism. By virtue of the normalisation constraint, we have  $p_3 = 1 - 3e_2$  and  $p_2 = 1 - 2e_2$ , and hence  $\mathcal{F} = e_2 - 4e_2^2$ ; referring to the  $N = 2$  row of Table I, we see that this is exactly  $\mathcal{M}_{AB}^{\text{lin}}/4$ . This is consistent with the fact that, for two qubits, Eq. (19) can be written as a function of a single entanglement invariant, which can be taken to be the concurrence. For two qutrits, however, the situation changes: Eq. (43) depends on more than the purity  $p_2 \equiv \text{Tr}(\rho_X^2)$ , and hence cannot be directly related to the concurrence alone. We also verify numerically that  $\mathcal{F}$  does not reproduce the value of  $\mathcal{M}_{AB}^{\text{lin}}/4$  implied by the  $N = 3$  formula. In fact, we find no linear relationship between  $\mathcal{M}_{AB}^{\text{lin}}$  and  $\mathcal{F}$  in the qutrit case. Thus, while non-local magic is tightly linked to entanglement diagnostics for two qubits, this equivalence appears tied to the paucity of inequivalent invariants for  $N = 2$ , and does not persist in general.

## V. CONCLUSIONS

We have developed an invariant-based construction of non-local magic for bipartite pure states of qudits and obtained compact analytic expressions for prime local dimensions  $N = 3, 5$ . Our results depend on the Schmidt-attainment hypothesis: that the non-local magic is manifest in the Schmidt-aligned family of states. Numerical

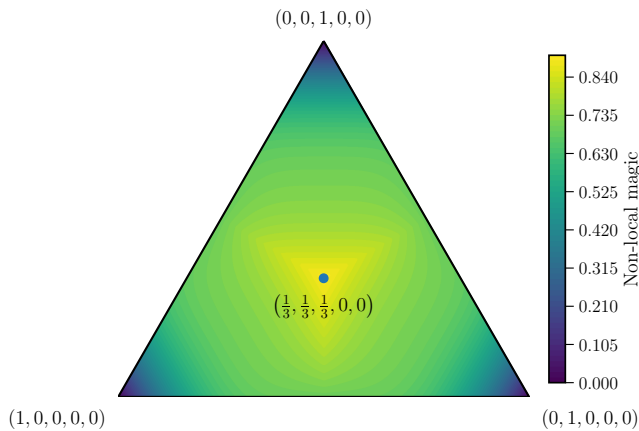


FIG. 2. Non-local magic for two ququints on the Schmidt-probability slice  $(\lambda_0^2, \lambda_1^2, \lambda_2^2, 0, 0)$ , where  $\sum_i \lambda_i^2 = 1$ . The colour scale shows the non-local magic  $\mathcal{M}_{N=5}$ . The plot is symmetric under permutations of  $(\lambda_0^2, \lambda_1^2, \lambda_2^2)$ , appearing as a threefold symmetric pattern over the triangular slice. The slice is chosen to feature the maximum value of  $\mathcal{M}_{N=5} = \ln(27/11) \approx 0.90$ , which occurs at  $\lambda_0^2 = \lambda_1^2 = \lambda_2^2 = 1/3$  (blue circle).

TABLE I. Closed-form expressions for  $\exp(-\mathcal{M}_N)$  for two-qudit systems of local dimension  $N$ . The  $N = 2, 3, 5$  rows are used to construct the NLM. The  $N = 4$  row is included only as a reference expression: our numerical checks show that the correspondingly constructed NLM does not reproduce the global local-unitary minimum in general.

$N$	$\exp(-\mathcal{M}_N)$
2	$1 - 4e_2 + 16e_2^2$
3	$1 - 2p_2 + 2p_2^2 + 4e_3s_1^2$
4	$3p_2^2 - 2p_4 + 120e_4 + 4c_{404} + 12c_{242} + 8c_{1331}$
5	$3p_2^2 - 2p_4 + 24e_5^{1/2}s_{111} + 24c_{2222} + 12c_{242} + 12c_{2204} + 8c_{1331} + 8c_{3113}$

comparisons between the Schmidt-based formulae and direct optimisation over  $U_A \otimes U_B$  show strong agreement for  $N = 3, 5$ . In contrast, for  $N = 4$  the analogous Schmidt-based expression does not reproduce the global minimum across parameter space, although it often remains close. We find that for systems of two qutrits, the maximum allowed non-local magic is  $\ln 2$ , while for ququints numerical scans indicate a maximal value consistent with  $\ln(27/11)$ . We also found that relations between the non-local magic and other diagnostics such as the concurrence and the anti-flatness of the entanglement spectrum, which were present for systems of two qubits, generally do not extend past  $N = 2$ . Overall, these results provide practical and largely analytic access to non-local magic in prime-dimensional two-qudit systems, and motivate a broader conjecture that Schmidt attainment persists for higher prime  $N$ .

## VI. ACKNOWLEDGEMENTS

We thank Gary Mooney and Cédric Simenel for useful discussions. All authors are supported by the Australian Research Council grant CE200100008. MJW is further supported by the Australian Research Council grant DP220100007. ENVW acknowledges the support he has received for this research through the provision of an Australian Government Research Training Program Scholarship.

### Appendix A: Comparison with numerical optimisation over local unitaries

Below we present numerical evidence to motivate what we have dubbed the Schmidt attainment hypothesis: that the minimisation over local unitaries defining the NLM is attained in the Schmidt-aligned family of states for  $N = 3, 5$ . This motivates our conjecture that Schmidt attainment holds for pairs of qudits of prime local dimension more generally.

To test this hypothesis, we sample  $10^4$  sets of Schmidt coefficients by drawing spectra  $\lambda \in \mathbb{R}_{\geq 0}^N$  uniformly on the positive orthant of the unit  $(N-1)$ -sphere and calculate (i) the value obtained from direct numerical minimisation over  $U_A \otimes U_B$ , and (ii) the value predicted by our formulae from Table I. The numerical minimisation is performed using the L-BFGS algorithm through Optax [37] with  $n_{\text{starts}} = 50$  ( $N = 3$ ), 200 ( $N = 4$ ), and 500 ( $N = 5$ ), using `maxiter` = 300 per start.

Fig. 3 shows this comparison for  $N = 3, 4, 5$ : the top row plots the result from our formula versus the numerically optimised values, while the bottom row histograms the residuals  $\mathcal{M}_{\text{formula}} - \mathcal{M}_{\text{numerical}}$ . For  $N = 3, 5$  almost all residuals are numerically indistinguishable from 0, with no positive residuals observed. Negative values are consistent with incomplete convergence of the numerical minimisation, which is more likely for the ququint scan for which the optimisation occurs over a much higher dimensional space.

For  $N = 4$ , by contrast, we find that the analogous Schmidt-based expression does not reproduce the global minimum throughout the full parameter space, although the prediction from our formula is usually a good estimate. The largest residual found is close to 0.12, and the distribution of absolute residuals is characterised by a mean of 0.01 and a standard deviation of 0.12. We find that about 72% of sampled points have residuals below 0.01, indicating that while the formula is often very close to the numerical minimum, a sizeable tail of larger deviations remains.

In order to better map the regions in  $\lambda^2$ -space in which the  $N = 4$  formula is trustworthy, we plot the residual  $\mathcal{M}_{\text{formula}} - \mathcal{M}_{\text{numerical}}$  on slices across fixed  $\lambda_3^2 \in \{0, 0.2, 0.4, 0.6\}$  in Fig. 4. For each value we select points in a narrow band  $|\lambda_3^2 - (\lambda_3^2)_*| \leq 0.02$ , normalise  $(\lambda_0^2, \lambda_1^2, \lambda_2^2)$  by  $1 - \lambda_3^2$ , and display the points on the canon-

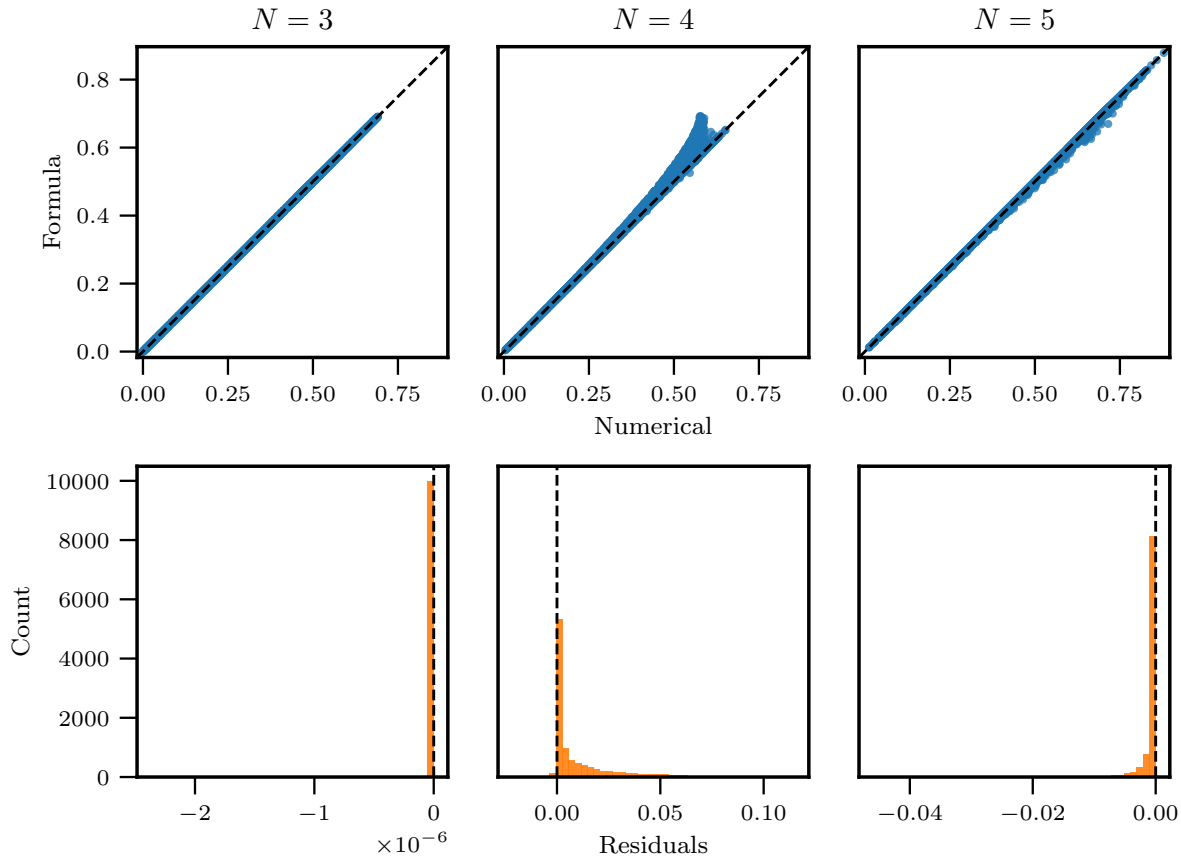


FIG. 3. Comparison of the non-local magic from direct numerical minimisation over  $U_A \otimes U_B$  and from the Schmidt-based formula for  $N = 3, 4, 5$ . For each  $N$ , we sample  $10^4$  points in Schmidt-parameter space and perform multi-start L-BFGS optimisation with  $n_{\text{starts}} = 50$  ( $N = 3$ ), 200 ( $N = 4$ ), and 500 ( $N = 5$ ), using `maxiter` = 300 per start. Top row: formula value versus numerically minimised value, with the dashed line showing equality. Bottom row: residual histograms for  $\mathcal{M}_{\text{formula}} - \mathcal{M}_{\text{numerical}}$ . Negative residuals are consistent with incomplete convergence of the numerical minimisation; positive residuals indicate formula values above the numerical minimum. For  $N = 3, 5$ , no positive residuals are observed in the sampled points, supporting Schmidt attainment in prime dimensions. For  $N = 4$ , positive residuals are present, showing that the analogous Schmidt-based expression does not reproduce the global minimum in general; nevertheless, it often lies close to the minimum.

ical simplex. In general, we find that the largest residuals occur at the boundary points of the space, where one of the  $\lambda_i$  vanishes. This is clearly evident in the  $\lambda_3^2 = 0$  slice, where large residuals are evident in much of the remaining parameter space, although points near the  $(\lambda_0^2, \lambda_1^2, \lambda_2^2)$ -subspace boundary still lead to trustworthy results. For larger values of  $\lambda_3^2$ , we continue to see that

the formula breaks down near the boundaries, where one of the  $\lambda_i^2$  vanishes. At  $\lambda_3^2 = 0.2$ , points on each edge near 0.5 appear to show smaller residuals, and hence better agreement, than points near 0.25 or 0.75, whereas for  $\lambda_3^2 \geq 0.4$  this trend seems to reverse. For  $\lambda_3^2 = 0.6$ , the points with large residuals are less localised to the boundaries than they are for  $\lambda_3^2 = 0.4$ .

- 
- [1] P. Gokhale, J. M. Baker, C. Duckering, F. T. Chong, N. C. Brown, and K. R. Brown, *IEEE Micro* **40**, 64 (2020).
- [2] D. Gottesman, in *22nd International Colloquium on Group Theoretical Methods in Physics* (1998) pp. 32–43, [arXiv:quant-ph/9807006](https://arxiv.org/abs/quant-ph/9807006).
- [3] D. Gottesman, (1997), [arXiv:quant-ph/9705052](https://arxiv.org/abs/quant-ph/9705052).
- [4] S. Aaronson and D. Gottesman, *Phys. Rev. A* **70**, 052328 (2004), [arXiv:quant-ph/0406196](https://arxiv.org/abs/quant-ph/0406196).
- [5] M. Beverland, E. Campbell, M. Howard, and V. Kliuchnikov, *Quantum Sci. Technol.* **5**, 035009 (2020), [arXiv:1904.01124](https://arxiv.org/abs/1904.01124) [quant-ph].
- [6] S. Bravyi and D. Gosset, *Phys. Rev. Lett.* **116**, 250501 (2016), [arXiv:1601.07601](https://arxiv.org/abs/1601.07601) [quant-ph].

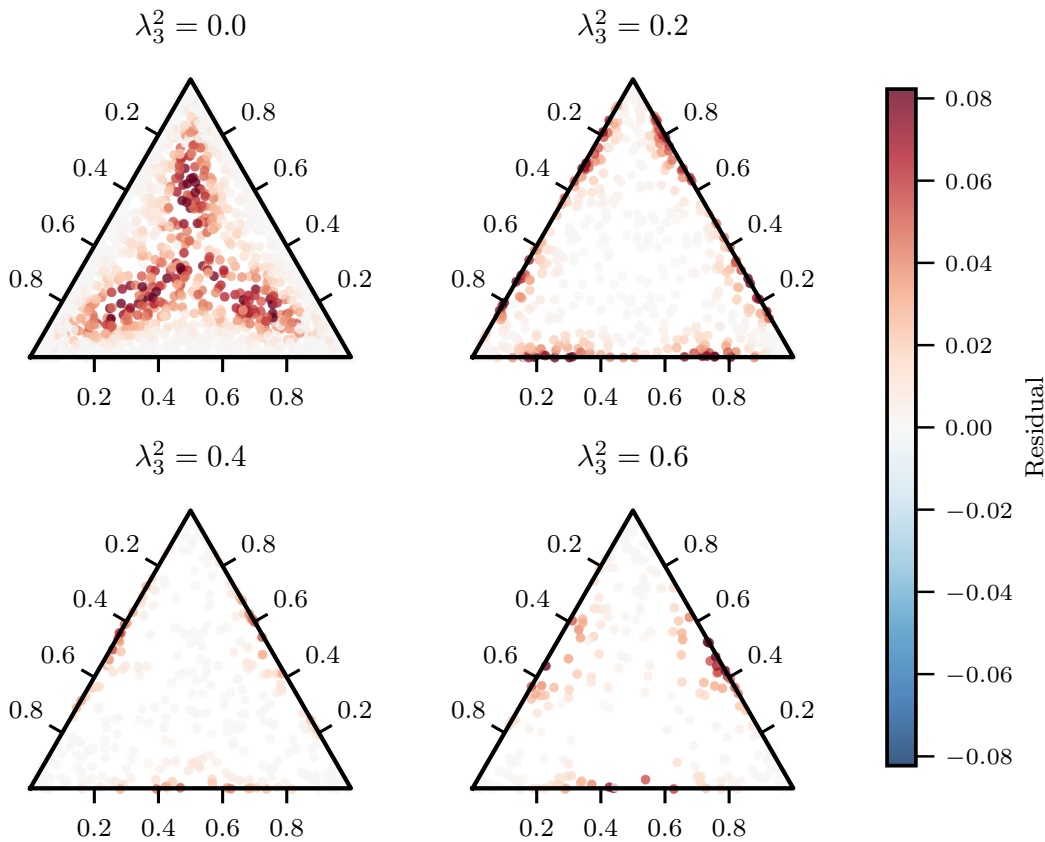


FIG. 4. Residual map for the  $N = 4$  Schmidt-based formula across projected slices of Schmidt-probability space. Shown is the residual  $\mathcal{M}_{\text{formula}} - \mathcal{M}_{\text{numerical}}$  for fixed  $\lambda_3^2 \in \{0, 0.2, 0.4, 0.6\}$ . For each panel, points are selected in a band  $|\lambda_3^2 - (\lambda_3^2)_*| \leq 0.02$ ; the remaining components  $(\lambda_0^2, \lambda_1^2, \lambda_2^2)$  are then normalised by  $1 - \lambda_3^2$ , and the data are plotted on the canonical simplex. The largest residuals occur near simplex boundaries, i.e. where one Schmidt component vanishes. At  $\lambda_3^2 = 0.2$  it seems that values along each boundary close to 0.5 are more trustworthy than those close to 0.25 or 0.75; the opposite appears true for  $\lambda_3^2 \geq 0.4$ . Very few points have negative residuals, and all such points are localised to the vertices, which represent  $(\lambda_0^2, \lambda_1^2, \lambda_2^2) = (1, 0, 0)$  and permutations.

- [7] S. Bravyi, D. Browne, P. Calpin, E. Campbell, D. Gosset, and M. Howard, *Quantum* **3**, 181 (2019), [arXiv:1808.00128 \[quant-ph\]](#).
- [8] S. Bravyi, G. Smith, and J. A. Smolin, *Phys. Rev. X* **6**, 021043 (2016), [arXiv:1506.01396 \[quant-ph\]](#).
- [9] S. Bravyi and A. Kitaev, *Phys. Rev. A* **71**, 022316 (2005), [arXiv:quant-ph/0403025](#).
- [10] K. Bu and D. E. Koh, *Phys. Rev. Lett.* **123**, 170502 (2019), [arXiv:1902.11257 \[quant-ph\]](#).
- [11] E. T. Campbell, *Phys. Rev. A* **83**, 032317 (2011), [arXiv:1010.0104 \[quant-ph\]](#).
- [12] A. Gu, S. F. E. Oliviero, and L. Leone, *Phys. Rev. A* **110**, 062427 (2024), [arXiv:2403.14912 \[quant-ph\]](#).
- [13] A. Gu, S. F. E. Oliviero, and L. Leone, *PRX Quantum* **6**, 020324 (2025), [arXiv:2403.19610 \[quant-ph\]](#).
- [14] A. Gu, H.-Y. Hu, D. Luo, T. L. Patti, N. C. Rubin, and S. F. Yelin, *Quantum* **8**, 1422 (2024), [arXiv:2308.11616 \[quant-ph\]](#).
- [15] Y. O. Nakagawa and Y. Lee, (2025), [arXiv:2508.14546 \[quant-ph\]](#).
- [16] Z.-W. Liu and A. Winter, *PRX Quantum* **3**, 020333 (2022), [arXiv:2010.13817 \[quant-ph\]](#).
- [17] J. R. Seddon, B. Regula, H. Pashayan, Y. Ouyang, and E. T. Campbell, *PRX Quantum* **2**, 010345 (2021), [arXiv:2002.06181 \[quant-ph\]](#).
- [18] S. True and A. Hamma, *Quantum* **6**, 818 (2022), [arXiv:2202.02648 \[quant-ph\]](#).
- [19] M. Yoganathan, R. Jozsa, and S. Strelchuk (2019) [arXiv:1806.03200 \[quant-ph\]](#).
- [20] S. Zhou, Z. Yang, A. Hamma, and C. Chamon, *SciPost Phys.* **9**, 087 (2020), [arXiv:1906.01079 \[cond-mat.stat-mech\]](#).
- [21] M. Bejan, C. McLauchlan, and B. Béri, *PRX Quantum* **5**, 030332 (2024), [arXiv:2312.00132 \[quant-ph\]](#).
- [22] D. E. Koh, *Quant. Inf. Comput.* **17**, 0262 (2017), [arXiv:1512.07892 \[quant-ph\]](#).
- [23] A. Bouland, J. F. Fitzsimons, and D. E. Koh (2018) [arXiv:1709.01805 \[quant-ph\]](#).
- [24] Y. Zhang and Y. Gu, (2024), [arXiv:2410.21128 \[quant-ph\]](#).
- [25] M. Howard and E. T. Campbell, *Phys. Rev. Lett.* **118**, 090501 (2017), [arXiv:1609.07488 \[quant-ph\]](#).
- [26] L. Leone, S. F. E. Oliviero, and A. Hamma, *Phys. Rev. Lett.* **128**, 050402 (2022), [arXiv:2106.12587 \[quant-ph\]](#).

- [27] D. Qian and J. Wang, *Phys. Rev. A* **111**, 052443 (2025), [arXiv:2502.06393 \[quant-ph\]](#).
- [28] C. Cao, G. Cheng, A. Hamma, L. Leone, W. Munizzi, and S. F. E. Oliviero, *PRX Quantum* **6**, 040375 (2025), [arXiv:2403.07056 \[hep-th\]](#).
- [29] C. Cao, *JHEP* **11**, 105, [arXiv:2306.14996 \[hep-th\]](#).
- [30] S. Cepollaro, S. Cusumano, A. Hamma, G. Lo Giudice, and J. Odavić, *Phys. Rev. D* **112**, 105012 (2025), [arXiv:2412.11918 \[quant-ph\]](#).
- [31] E. Tirrito, P. S. Tarabunga, G. Lami, T. Chanda, L. Leone, S. F. E. Oliviero, M. Dalmonte, M. Collura, and A. Hamma, *Phys. Rev. A* **109**, L040401 (2024), [arXiv:2304.01175 \[quant-ph\]](#).
- [32] C. E. P. Robin and M. J. Savage, (2025), [arXiv:2510.23426 \[quant-ph\]](#).
- [33] I. Chernyshev, C. E. P. Robin, and M. J. Savage, *Phys. Rev. Res.* **7**, 023228 (2025), [arXiv:2411.04203 \[quant-ph\]](#).
- [34] J. Thaler and S. Trifinopoulos, *Phys. Rev. D* **111**, 056021 (2025), [arXiv:2410.23343 \[hep-ph\]](#).
- [35] R. Horodecki and M. Horodecki, *Phys. Rev. A* **54**, 1838 (1996), [arXiv:quant-ph/9607007](#).
- [36] J. Schlienz and G. Mahler, *Phys. Rev. A* **52**, 4396 (1995).
- [37] DeepMind, I. Babuschkin, K. Baumli, A. Bell, S. Bhupatiraju, J. Bruce, P. Buchlovsky, D. Budden, T. Cai, A. Clark, I. Danihelka, A. Dedieu, C. Fantacci, J. Godwin, C. Jones, R. Hemsley, T. Hennigan, M. Hessel, S. Hou, S. Kapturovski, T. Keck, I. Kemaev, M. King, M. Kunesch, L. Martens, H. Merzic, V. Mikulik, T. Norman, G. Papamakarios, J. Quan, R. Ring, F. Ruiz, A. Sanchez, L. Sartran, R. Schneider, E. Sezener, S. Spencer, S. Srinivasan, M. Stanojević, W. Stokowiec, L. Wang, G. Zhou, and F. Viola, *The DeepMind JAX Ecosystem* (2020).